HAL
open science

ERRα expression in bone metastases leads to an exacerbated anti-tumor immune response

Mathilde Bouchet, Alexandra Lainé, Cyril Boyault, Mathilde
Proponnet-Guerault, Emmanuelle Meugnier, Lamia Bouazza, Casina E Kan,
Sandra Geraci, Soumaya El-Moghrabi, Hector Hernandez-Vargas, et al.

▶ To cite this version:

HAL Id: hal-02642369
https://hal.science/hal-02642369

Submitted on 28 May 2020

ERRα expression in bone metastases leads to an exacerbated anti-tumor immune response

Mathilde Bouchet[1,2,3*], Alexandra Lainé[4,2*], Cyril Boyault[5], Mathilde Proponnet-Guerault[5], Emmanuelle Meugnier[6], Lamia Bouazza[1,2], Casina W. Kan[7], Sandra Geraci[1,2], Soumaya El-Moghrabi[1,2], Hector Hernandez-Vargas[4], Claire Benetollo[2,8], Yuji Yoshiko[9], Martine Duterque-Coquillaud[10], Philippe Clézardin[1,2], Julien C. Marie[4,2] and Edith Bonnelye[1,2,11]

[1] INSERM-UMR1033, Labex DEVweCAN, F-69008, Lyon-France.
[2] University of Lyon-France
[3] IGFL, Lyon-France (present address)
[4] Department of immunology virology and inflammation, INSERM-UMR1052 CNRS 5286-Centre Léon Bérard, Labex DEVweCAN, F-69008, Lyon-France
[5] Institute for Advanced Biosciences, UMR5209-INSERM1302, La Tronche-France
[6] INSERMU1060-INRA-U1397, Lyon-France
[7] INSERM-UMR1033, Lyon-France.
[8] INSERM-UMR5292 INSERM U1028, Lyon-France
[9] Department of Calcified Tissue Biology, Hiroshima University, 1-2-3 Kasumi, Minami-ku, Hiroshima 734-8553, Japan
[10] CNRS-UMR9020-INSERM-UMR1277-University of Lille-Institut Pasteur de Lille-France
[11] Current Address: CNRS ERL 6001/ INSERM U1232, Institut de Cancérologie de l'ouest, ICO, 44805 Saint-Herblain cedex
*These authors contributed equally to this work

Running title: Immunomodulatory function of ERRα in bone metastases

Address correspondence to: CAN-19-3584
Edith Bonnelye
CNRS ERL 6001/INSERM U1232
Institut de Cancérologie de l'ouest
Bd Jacques Monod -44805 Saint-Herblain-France
33+2 53 48 47 81
edith.bonnelye@inserm.fr

Julien C. Marie, PhD
Department of Tumor Escape Resistance Immunity
C R C L-Bat Cheney B 4eme étage
28 rue Laennec-69373 Lyon cedex 08-FRANCE
33 + 4 26 55 67 48 (office)
julien.marie@inserm.fr

Conflict of interest statement: The authors declare no potential conflicts of interest.

Statements of significance

This study places ERRα at the interplay between the immune response and bone metastases of breast cancer, highlighting a potential target for intervention in advanced disease.

Abstract (150 words)

Bone is the most common metastatic site for breast cancer. Although the estrogen-related receptor alpha (ERRα) has been implicated in breast cancer cell dissemination to the bone from the primary tumor, its role after tumor cell anchorage in the bone microenvironment remains elusive. Here, we reveal that ERRα inhibits the progression of bone metastases of breast cancer cells by increasing the immune activity of the bone microenvironment. Overexpression of ERRα in breast cancer bone metastases induced expression of chemokines CCL17 and CCL20 and repressed production of transforming growth factor beta 3 (TGF-β3). Subsequently, CD8^{+} T lymphocytes recruited to bone metastases escaped TGF-β signaling control and were endowed with exacerbated cytotoxic features, resulting in significant reduction in metastases. The clinical relevance of our findings in mice was confirmed in over 240 breast cancer patients. Thus, this study reveals that ERRα regulates immune properties in the bone microenvironment that contributes to decreasing metastatic growth.

Introduction

Bone metastases (BM) are a frequent complication of cancer, occurring in up to 70 percent of patients with advanced breast cancer (BCa), and are associated with both high morbidity and elevated mortality (1)(2)(3). The progression of BM relies on the ability of the malignant cell colonizing the bone and to modify bone micro-environment allowing the release of bone-stored factors including transforming growth factor (TGF-β), bone morphogenetic protein (BMP) or insulin growth factor (IGF), which in turn stimulate BM progression (2)(4). However treatments which mainly involved anti-resorptive agents of the bone failed to improve the overall survival of cancer patients even though it inhibited osteoclasts resorptive activity (3), implying that other mechanisms than the activation of osteoclasts by tumor cells are involved in modulating BM growth. The immune cells present in the bone, and particularly activated CD8$^+$ T lymphocytes can repress the progression of BCa osteolytic BM (5)(6)(7)(8). However, whether BM can influence the activation of immune cells present in the bone and by which mechanisms is totally unknown.

The estrogen-related receptor alpha (ERRα, or NR3B1 according to the Nuclear Receptors Nomenclature Committee, 1999) is over expressed in 55% of breast tumors (9)(10). Though ERRα shares structural similarities with the estrogen receptors α/β, it does not bind estrogens and no natural ligand has yet been found (11), though several molecules can either increase or decrease ERRα activity, such as the inverse-agonists XCT790 or C29 (12)(13). ERRα is mainly involved in the adaptive bioenergetics response (11). In cancer, beside angiogenesis, ERRα is strongly linked to tumor cell-invasion (14)(15). Notably, ERRα-positive tumors are associated with more invasive BCa and a higher risk of recurrence (9)(14). The over-expression of ERRα in BCa promotes tumor growth in the mammary gland and BCa metastatic dissemination to the bone (16). However, the role of ERRα in BM outcome once they are anchorage in the bone microenvironment remains elusive.

In this study, using loss and gain of expression of ERRα, as well as chemical inhibitors, we demonstrated that ERRα enhanced the ability of BCa cell established in the bone to recruit activated CD8^{+} T cells to the bone. In addition, ERRα expression on BCa cells repressed their ability to produce TGF-β, a potent immune-suppressive cytokine. Subsequently, TGF-β signaling was impaired in T cells infiltrating the bone, and CD8^{+} T cell cytotoxic function exacerbated leading to metastatic progression. Altogether, our work assigns a totally unexpected role to ERRα, revealing that the expression of this orphan receptor on the BCa metastases promotes an efficient anti-tumor immune response once the tumor cells are settled in bone.

Materials and Methods

Cell lines

The mouse triple negative breast (TNBC) cancer cell line 4T1 (year 2012) (ATCC lot: 58603185-CRL-2539) and human luminal MCF7 (year 2012) (ATCC-HTB-22 Lot: 86012803) were obtained from the American Type Culture Collection. MDA-MB-231/BO2-FRT (BO2) BCa cells, a subpopulation of the human MDA-MB-231 BCa line (TNBC) was selected for their high efficiency to metastasize to bone (17). These cell line was tested for authentication by DNA fingerprinting using short repeat (STR) method in 2014. TNBC cell lines and MCF7 were cultured in DMEM or RPMI-1640 (Life-Technologies) medium, respectively, supplemented with 10% fetal bovine serum (FBS, Perbio) and 1% penicillin/streptomycin (Invitrogen) at 37°C in a 5% CO_2 incubator. Cells lines were tested for mycoplasma regularly. Mouse and human *ESRRA* cDNA (ERRα) and the dominant-negative co-activator domain AF2 (AF2) mutant were described previously (16)(18). Briefly, pSRα-ERRαWT and pEcmv-ERRαAF2 or respective empty vectors (CT) constructs were transfected into parental 4T1 cells and cultured for 4 weeks in puromycin (2 μg/mL) (Life-Technologies). Three independent clones were obtained from pSRα-ERRαWT transfection (4T1-ERRα) and from pEcmv-ERRαAF2 transfection (4T1-

ERRαAF2). Two independent clones were obtained from empty vectors transfection respectively pSRα-4T1-CT (4T1-CT) and pEcmv-4T1-CT (4T1-CTaf2). For MCF7 clones, a mix containing 1.5μg Retroviral pLPCX-Human-ERRαWT, pLPCX-HumanERRαAF2 or empty vector and 0.5μg pCMV-VSV-G envelope vector (Cell-Biolabs) were used previously (16). 4T1-ERRα and 4T1-ERRαAF2 (pool of 3clones each) cells were treated for 24 hours with the ERRα inverse-agonists XCT790 (Sigma) or C29 (AGVdiscovery, France) at 1μM and 5μM, respectively, as described (13) (16) (19). DMSO was used as a vehicle (Veh).

Animal studies

6-week-old BALB/c female mice were purchased from Janvier (France) and housed in a SPF facility (ALECS platform (Faculté de Médecine Laennec, Lyon, France). BM experiments were performed by inoculating intra-arterially either 4T1-CT (pool of 2 clones) in parallel with 4T1-ERRα (pool of 3 clones), or 4T1-CT(af2) (pool of 2 clones) in parallel with 4T1-ERRαAF2 (pool of 3 clones) cell lines (5×10^5 cells in 100 μL of PBS). Radiographs (LifeRay HM Plus, Ferrania) of animals were taken at 15 days after inoculation using X-ray (MX-20; Faxitron X-ray Corporation). The extent of bone destruction for each animal was expressed in mm^2. Animals were sacrificed and hind limbs were then collected for histology and histomorphometric analysis. Tibiae were scanned using microcomputed tomography (Skyscan1076, Skyscan, Belgium) with an 8.8 voxel size and an X-ray tube (50 kV; 80 mA) with 0.5 μm aluminum filter and three-dimensional reconstructions were performed with a dedicated visualization software (NRecon&CTVox, and Skyscan) (18). Bone Volume/Tissue Volume: (%BV/TV) were carried out with CTAn (version 1.9, Skyscan) and CTVol (version 2.0, Skyscan) software. Dissected bones were then processed for histological (Goldner's Trichrome solution staining) and histomorphometric analyses (tumor burden-to-soft tissue volume (%TB/STV)) (18). Depletion of $CD8^+$ T cells was performed by intra-peritoneal injection of anti-CD8β (BioXCell, clone Lyt3.2;

BE0223). 387.5 µg per mouse were injected 4 times every two days, from day 10 after metastasis injection *i.e* when osteolytic lesions start to be detectable.

Ethics statement

Mice were handled according to the French Ministerial Decree No.87-848 of 19 October 1987. Experimental protocols were approved by the Institutional Animal Care and Use Committee at the Université-Lyon1 (France) (ethic committee CEEA-55 Comité d'Ethique en Expérimentation Animale-DR2014-44-DR2015-28).

Human sample meta-genomic analysis

Correlation analysis were performed using published datasets downloaded from the Gene-Expression-Omnibus including primary tumor, no-metastases, Visceral+bone or only BM (GSE12276-GSE2034-GSE2603) (n=248) (20)(21)(22). Z-scores were calculated on normalized data of each dataset by subtracting the population mean from individual expression values for each gene and then dividing the difference by the population standard deviation.

Sign arrays

The expression levels of several chemokines known to influence T cell chemo-attraction were obtained by qPCR Sign Arrays (Cytokines Array and Inflammation Array). Indeed, two qPCR Sign Arrays: Cytokines and Inflammation Arrays (AnyGenes, CT1M1-IFM1)(CliniSciences) were used to quantify expression of cytokines, chemokines and growth factors. Total RNA was extracted from 4T1-CT and 4T1-ERRα cells and 2 µg were reverse-transcribed as previously described (16). Real-Time PCR was performed according to the manufacturer's instructions. Two heat maps were generated using the heatmap.2 function in the gplots library of R (version 3.5.1). Only regulations that were reproducible between the two arrays are presented.

Protein-protein interaction network reconstruction and analysis.

The protein-protein interaction network with BIOGRID (release 3.4.160) from *Homo sapiens* with PSICQUIC (Proteomics-Standard-Initiative-Common-QUery-InterfaCe) retrieval (10242018) and Cytoscape environment was used (16). A BIOGRID (https://thebiogrid.org/)-based custom approach was used to define a protein interactome of the following proteins: ESRRA-CCL17-CCL20-OPG-NRIP1-SRC1-SRC2-SRC3-PGC1A-PGC1B-CCR4 and CCR6. The resulting interactome encompasses 911 proteins (hereby defined as "Extended Network of ESRRA, CCL17, CCL20") (reachable on Ndex webserver here) (Supplementary Fig.S1). To determine the connectors between CCL17, CCL20 and ESRRA, a custom approach combining shortest path and connectivity degree analysis was applied to determine a "Minimal Network of ESRRA, CCL17, CCL20" (reachable on Ndex webserver here) (containing 101 proteins) acknowledging connections that may support ESRRA signaling (Supplementary Fig. S2) (16). We overlaid and extracted information from the Gene-Ontology-consortium to pinpoint proteins that are already known to be involved in the immune system process, as well as T and B cell homeostasis (GO-IDs: 0002376, 0043029, 0001782) to create "Minimal Network specific to immune response to tumor" (containing 52 proteins). To determine the connectors between ESRRA and CCL17, ESRRA and CCL20, a shortest path was applied to the "Minimal Network of ESRRA, CCL17 and CCL20" (16)(23)(24).

Ex vivo cell preparation

For hind limbs, muscles were removed and bones were sliced, then incubated at 37°C with a 1/10 solution of collagenase hyaluronidase (Stem cell) for 2 hours. Bones were then mechanically disrupted with a syringe plunge, filtered and cells were collected. For lung metastases (LM), lungs were crushed with a syringe plunge on a filter (100 μm) (BD Bioscience) and cells were collected. Cells released from lungs and bones were incubated at 37°C in the presence of DMEM (Life Technologies) supplemented with 10% (v/v) fetal bovine serum (Perbio/Thermo Scientific)

and 6-thioguanine (Sigma A4882) (10 μg/mL) for 2 weeks. The cells were then counted after being stained using Crystal Violet (RAL diagnostic 317980).

Flow Cytometry

Cells from spleen and lungs, obtained after mechanical disruption, and flushed bone marrow cells were pre-incubated with anti-CD16/32 (93 clone, Biolegend) and stained for surface marker for 30 minutes at 4°C with the following antibodies: anti-CD45 (30-F11 clone, BD or eBiosciences), anti-CD3e (145-2C11 clone, BD), anti-CD4 (GK1.5 clone, BD), anti-CD8 (53-6.7 clone, BD or eBiosciences), anti-CD19 (1D3 clone, BD), anti-CD11b (M1/70 clone, eBiosciences), anti-CD11c (N418 clone, eBiosciences), anti-CCR4 (2G12 clone Biolegend) anti-CCR6 (29-2217clone Biolegend), anti-Ly6C (AL21 clone, BD), anti-Ly6G (1A8 clone, BD), anti-F4/80 (BM8 clone, Biolegend), anti-CD107a (LAMP-1)(1D4B clone, BD), anti-FasL (MFL3 clone, eBiosciences). For cytokine production, cells were first incubated for 4 hours with PMA (P1585-1MG, Sigma), Ionomycin (I0634-1MG, Sigma) and Brefeldin A (00-4506-51, Life Technologies). Intracellular staining was performed with the Transcription Factor Staining Buffer Set (00-5523-00, eBiosciences), according to manufacturer's recommendations. The following antibodies were used: anti-Foxp3 (R16-715 clone, BD), anti-IFN-γ (XMG1.2 clone, BD), anti-GzA (GzA-3G8.5 clone, eBiosciences), anti-GzB (GB11 clone, Invitrogen), anti-Ki67 (11F6 clone Biolegend), anti-pSMAD2/3 (D27F4 clone, Cell Signalling) coupled with anti-rabbit A488. CD8$^+$ T cell depletion was checked by flow cytometry on metastatic bone marrow and spleen using anti-CD8α (53-6.7 e-Biosciences). Data were acquired on a LSR-II (BD Biosciences) and analyzed with the FlowJo software version X.

Determination of ERRα binding sites

The analysis of ERRα binding sites on TCA AGGTCA promoter regions was performed using the GTRD ("Gene Transcription Regulation Database") that includes ChIP-seq data (http://gtrd.biouml.org/)(25).

Chromatine immunoprecipitation (ChIP)

ChIP assays were performed as previously described (16) from MDA-MB231-B02-CT and -ERRα cells (18) using either a monoclonal rabbit anti-ERRα(13826)(Cell-Signaling) or a control rabbit IgG(2729) antibody (Cell-Signaling). The immune-precipitated genomic DNA was purified using NucleoSpin Clean-up colums (Macherey-Nagel,Germany) and analyzed by qPCR. Quantification of ChIP enrichment was calculated relative to input values. Distal and proximal elements of ERRα gene were used as negative and positive controls respectively (26).

Histology-Immunocytochemistry

Tibia bearing metastases as well as lungs were fixed in 4% PFA (paraformaldehyde) (Antigenfix Diapath P0014), embedded in paraffin (Histowax Histolab 00403) then cut (5μm sections) on a microtome (Microm HM 350S). Immunocytochemical analyses were performed by incubating tissue sections overnight with goat polyclonal antibody *ERRα* (V-19, Santa Cruz) (1/40), rabbit polyclonal anti-human/mouse *CCL17* (PA5-34515, ThermoFisher) (1/100), rabbit polyclonal anti-mouse *CCL20* (ab139585, Abcam) (1/100), rabbit polyclonal anti-human/mouse activated *TGF-β3* (ab15537, Abcam) (1/100). Sections were then incubated with HRP-conjugated anti-mouse (K4000, Dako) and anti-rabbit (K4002, Dako) according to the manufacturer's recommendations or anti-goat (sc2020, Santa Cruz)(1/300) antibodies for 1 hour and were detected using 3,3'-diaminobenzidine (K3467, Dako) according to the manufacturer's instructions. Counterstaining was performed using Mayer's hematoxylin (Merck) according the supplier's protocol. Lungs sections were made at three different depths for each mouse and stained with H&E. Metastasis counting was performed in double blind.

TUNEL assay

Bone sections were deparaffinized and rehydrated followed by permeabilization with 0.2% triton (T9284, Sigma) and digestion with proteinase K (1µg/mL) (K182001, ThermoFisher). For positive control, sections were incubated with DNAse I at 1mg/mL (Sigma, 11284932001). Sections were then incubated with biotin-16-dUTP (Sigma, 11093070910) and TUNEL enzyme (Sigma, 11767305001) in deoxynucleotidyltransferase buffer (Tris-HCl 125mM (Euromedex, EU0011), sodium cacodylate 200mM (Sigma, C0250), BSA 6mM (Sigma, A7906), $CoCl_2$ 1mM (Sigma, 15862-1ml-F)) at 37°C for 60 minutes in a humid atmosphere. Sections were washed in stop buffer (300mM NaCl (Sigma, S3014), 30mM $NaC_6H_5O_7$-sodium citrate (Sigma, 71406)) and blocked with 2% BSA (Sigma, A7906). Sections were then labelled with streptavidin-phycoerythrin (PE) (eBiosciences, 12-4317-87) and DAPI (Euromedex, 1050-A) and mounted with Fluoromount (Sigma, F4680-25ml) (upright microscope zeiss axioimager (sip 60549)).

Real time RT-PCR

Total RNAs from three independent batches of each clone of 4T1, MCF7 and B02 cell (CT, ERRα and ERRαAF2) were extracted with Trizol-reagent (Life-Technologies) and 2µg were reverse-transcribed using qScript^{TM} cDNA SuperMix (Quanta-Biosciences). Real-time PCR was performed on a Mastercycler-ep-Realplex (Eppendorf) with primers specific to human and mouse genes (Supplementary Table S1) using Quantifast-SYBR-Green (Life-Technologies) according to the manufacturer's instructions. The ribosomal protein *RPL32 (L32)* gene was used as a housekeeping gene for quantification and relative results expressed as fold differences equal to $2^{-\Delta\Delta Ct}$.

Statistical analyses

Data were analyzed statistically using either the non-parametric Mann-Whitney U test or unpaired t-test for *in vivo* studies (n = 10 mice for each group (bioStaTGV), unblinded studies). *In vivo* data

on bone were confirmed (n = 3) on smaller groups (n = 4). *In vitro* assays were repeated at least twice and performed on triplicate samples. Data were analyzed using ANOVA and paired Student t-test to assess the differences between groups. All data are presented as means ± SEM with similar variances between groups. Correlation scores for meta-analysis were calculated using the Pearson-correlation-coefficient. Statistical significance was determined by GraphPad Prism v5.02 using the two-sided Student t-test. All statistical analyses were performed using the GraphPad Prism software (San Diego, USA). P-values less than 0.05 were considered statistically significant.

Results

ERRα expression in BCa cells inhibits metastases growth in bones

In order to assess the role of ERRα in BCa cells after tumor cell-anchorage in the bone microenvironment, BALB/c mice were intra-arterially injected with first a pool of three independent 4T1 tumor cell clones over-expressing-ERRα (4T1-ERRα), and a pool of two 4T1 tumor cell clones transfected with empty vector controls (4T1-CT) (16). Remarkably, fifteen days later, radiographic analysis revealed that animals bearing 4T1-ERRα tumors had osteolytic lesions that were 70% smaller than those of mice bearing 4T1-CT tumors (9.39 ± 2.6 *vs* 3.08 ± 1.45 mm^2) (**Fig. 1A,B**). The inhibitory effect of ERRα on BCa cell growth was associated with mild bone destruction (**Fig. 1C-E**). Histological and histomorphometric analyses also demonstrated the limitation of BM progression when BCa cells over-expressed ERRα (**Fig. 1F,G**). In clear contrast, when clones expressing a dominant-negative form (4T1-ERRαAF2) with their respective controls clones (4T1-CTaf2) were injected later, we found a 60% increase in osteolytic lesions in animals bearing ERRαAF2 tumors compared to control (4T1-CTaf2) mice (3.82 ± 1.99 *vs* 9.27 ± 2.064 mm^2) leading to their earlier sacrifice, prior 4T1-CT(af2) BM reach the percentage of osteolysis observed in 4T1-CT (**Fig. 1H,I**). Concomitantly, increased bone destruction and tumor burden

was observed (**Fig. 1J-N**). Given that 4T1 cells also colonize the lung (16), we analyzed the effects of ERRα expression on the development of LM. As opposed to the bone, both numbers of LM and numbers of BCa colonies extracted from the lungs were independent of the expression levels of ERRα in 4T1 cells (**Fig. 2A-F**). Of note, the ERRα over-expression in LM was observed in animals bearing 4T1-ERRα tumors compared to control groups (**Fig. 2G**). Taken together, this first set of data reveals that the over-expression of ERRα in BCa cells prevents their growth in the bone, and suggests that ERRα expression in BCa may affect the bone microenvironment to prevent BM progression.

ERRα expression in BCa cells increases T cell anti-tumor response in the bone

Given the importance of the immune response in the control of tumor growth, in particular metastases (5)(6)(7)(8), we next analyzed the effects of the expression of ERRα by BCa cells on the bone immune system. It is worth noting that no significant effect was observed on innate cells including dendritic cells, macrophages, with the exception of slight decrease in neutrophils (15%) in the bone colonized by 4T1-ERRα compared to 4T1-CT cells (Supplementary Fig. S3A-C). However, we found that metastatic legs of animals bearing 4T1-ERRα tumors contained 5 times more T cells than those colonized with 4T1-CT cells (**Fig. 3A**). Moreover, in line with the larger 4T1-CT BM observed (**Fig. 1**), which developed at the expense of the bone marrow that is largely depicted to sustain all stages of B cell medullary development (7)(8), the CD19$^+$ compartment was 4-5 times lower in mice bearing 4T1-CT BM compared to 4T1-ERRα BM (**Fig. 3A**). Of note, T cell enrichment was neither observed in the lungs where 4T1-ERRα cells were also anchored (**Fig. 3B**), nor in the none invaded lymphoid organs such as the spleen (Supplementary Fig. S3 D,E), implying that the expression of ERRα in BCa cells affected the T cell homeostasis after their anchorage in the bone. Interestingly, the increase in T cell proportion after 4T1-ERRα cell bone settlement was largely restricted to the CD8$^+$T lymphocyte compartment, with a 3.5-fold increase

in their number and percentage in bones bearing 4T1-ERRα tumors compared to bone colonized with 4T1-CT cells (**Fig. 3A**), whereas the proportion of CD4$^+$T cells in the bone, including that of Foxp3$^+$ regulatory T (Treg) cells was unaffected (Supplementary Fig. S3C).

In order to further characterize the CD8$^+$ T cells over-represented in the bone after 4T1-ERRα cell colonization, we then analyzed their ability to produce cytotoxic molecules and cytokines. Strikingly, in bone colonized with 4T1-ERRα cells, we found that CD8$^+$ T cells expressed higher levels of FasL, Granzyme (Granz) A and B, in association with LAMP1 at their cell surface as well as IFN-γ whereas these molecules were barely detectable in CD8$^+$ T cells from bones bearing 4T1-CT cells (**Fig. 3C-E**). In total agreement with this exacerbated cytotoxic program of CD8$^+$ T in the presence of 4T1-ERRα BCa cells in the bone, we found that a large fraction of 4T1-ERRα BM underwent apoptosis compared to 4T1-CT cells (**Fig. 3F,G**). No exacerbated sign of cytotoxic activity was observed in the non-invaded spleen or in the metastatic lungs of mice bearing 4T1-ERRα cells (Supplementary Fig. S4A). Importantly, the depletion of CD8$^+$ T cells was sufficient (**Fig. 4A**) to increase 4T1-ERRα BM progression (**Fig. 4 B-E**). This set of data suggests that the expression of ERRα in BCa cells influences the CD8$^+$ T cell homeostasis and increases their anti-tumor cytotoxic program in the bone allowing the control of the tumor progression.

ERRα expression leads to high levels of CCL17 and CCL20 production in BCa cells

The aforementioned data strongly suggest that the expression of ERRα by BCa cells influences the bone microenvironment to promote an efficient anti-tumor response. Interestingly, we failed to find any difference in Ki67 staining between CD8$^+$T cells evolving with either 4T1-CT or 4T1-ERRαBM (Supplementary Fig. S4B), suggesting that ERRα expression affected T cell-recruitment to the bone rather than their proliferation in the bone. In order to address this hypothesis, we monitored the expression levels of several chemokines known to influence T cell

chemo-attraction and found a 2- and 3-fold up-regulation of *Ccl17* and *Ccl20* in 4T1-ERRα cells, respectively (**Fig. 5A,B**, Supplementary Fig. S5A, Table S2). C29 or XCT-790 were sufficient to inhibit the over-expression of both *Ccl17* and *Ccl20*, while no effect was observed in 4T1-ERRαAF2 cells ruling out any off-target effects (**Fig. 5C-D**; Supplementary Fig. S5B-C) (27), arguing in favour of a direct role for ERRα in the control of the expression of these two chemokines (13). Of note, the ability of ERRα to up-regulate *Ccl17* and *Ccl20* was also observed in other BCa cells including MCF7 and MDA-MB-231-B02 cells (Supplementary Fig. S5D-E) (16)(18). Interestingly, the up-regulation of CCL17 and CCL20, at both gene and protein levels due to ERRα over-expression was sustained in 4T1-ERRα BM (**Fig. 5E,F**) but lost in LM (Supplementary Fig. S5F). This data was reinforced following the analysis of ChIP-seq data revealing binding site for ERRα in the promoter of *Ccl17* and in *Ccl20* (Supplementary Fig.S6A-D).

Given that CCL17 and CCL20 were reported to attract the fraction of activated CD8^{+} T cells expressing CCR4 and CCR6 (28), we next monitored the expression of both chemokine receptors on CD8^{+} T cells from the bone of animals bearing BM. In total agreement with the ability of 4T1-ERRα cells to sustain their production of CCL17 and CCL20 in the bone, and the activated phenotype of CD8^{+} T cells (**Fig. 3**), we found that, in bone colonized by 4T1-ERRα, a large fraction of CD8^{+} T cells expressed either CCR4 or CCR6 or both (**Fig. 5G**). Thus, BCa cells over-expressing ERRα are endowed with a unique ability to produce high amounts of CCL17 and CCL20 and efficiently recruit activated CD8^{+} T cells to the bone.

ERRα expression in BCa cells reduces their TGF-β3 production and decreases TGF-β signaling in BM

Since the cytotoxic program of CD8^{+}T cells was largely exacerbated in legs bearing 4T1-ERRα cells, we next assessed the mechanisms by which ERRα over-expression in BCa cells increased their cytotoxic function in the bone. To this end, we further investigated the connection

between CCL17-CCL20 and *ERRα* (*ESRRA*) by choosing a global approach combining bioinformatic analyses of protein interaction networks and transcriptional regulator databases (Supplementary Fig. S1:extended network -S2:minimal network) (29). We created the "Minimal Network specific to immune response to tumor" (containing 52 proteins) (**Fig. 6A**) and by shortest path analysis, we then identified two new ESRRA-CCL17 or ESRRA-CCL20-associated regulators: VCAM and TGF-β3 (**Fig. 6B,C**). We and others reported that *TGF-β* signalling in T cells inhibits the cytotoxic differentiation program of CD8^{+} T cells both in humans and mice (30)(31), we thus focused on this cytokine. The analysis of *Tgf-β3* expression revealed a 70% decrease in 4T1-ERRα compared to 4T1-CT cells (**Fig. 6D**). *Ex vivo* bone cultures confirmed that ERRα up-regulation in BCa cells negatively regulates *Tgf-β3* expression with a 55% decrease compared to control BCa BM (**Fig. 6E**). Strikingly, immunohistological staining revealed that the production of TGF-β3 was largely decreased in BCa BM over-expressing ERRα (**Fig. 6F**). In agreement with the decrease of *Tgf-β3* expression in 4T1-ERRα , we observed an increase in TGF-β3 levels in 4T1-ERRαAF2 BM (**Fig. 6D**) and a 5-fold increase in *Tgf-β3* expression after treatment of 4T1-ERRα cells with the inverse agonist XCT-790 (**Fig. 6G**). Similar results were observed in MCF7 and MDA-MB-231-B02 human cell lines (**Fig. 6H**), ruling out an effect restricted to mouse 4T1 cells. Altogether these results reveal that the over-expression of ERRα represses the expression of TGF-β3 in BCa and could thus prevent the BCa BM from creating an immunosuppressive microenvironment provided by TGF-β signal activation in immune cells.

In order to unconditionally confirm that CD8^{+}T cell evolving in 4T1-ERRα colonized bone escape TGF-β signaling control, we next analyzed CD8^{+}T cells from metastatic legs for the phosphorylation of SMAD2/3 proteins which translates specifically the TGF-β signaling activation (32). Clearly, SMAD2/3 phosphorylation was 2-3 times lower compared to that of CD8^{+} T cells from 4T1-CT metastatic legs (**Fig. 6I**). Thus, in addition to increasing CD8^{+}T cell

recruitment to the bone, ERRα over-expression in BCa cells impairs their ability to produce high amounts of TGF-β3, decreasing TGF-β signaling in CD8$^+$T cells, a key repressor of their cytotoxic activity and capacity to eliminate cancer cells.

Over-expression of ESRRA (Errα) in patient tumours is associated with high levels of CCL17 CCL20 and low levels of TGF-β3 expression

Finally, we addressed the relevance of our data obtained in mice to the human pathology. We performed a meta-analysis on 248 patients including luminal and triple-negative breast tumors (TNBC) split into four groups: all tumors (n = 248), patients without metastases (No Mets, n = 121), patients that had visceral and bone metastases (Visceral+Bone metastases, n = 53) and patients that had only bone metastases (Bone Only, n = 74). As in mice, the *ESRRA (Errα)* expression was positively correlated with that of *CCL17* and *CCL20* and inversely proportional to that of *TGF-β3* in patients with metastases restricted to the bone (Bone Only) with luminal and TNBC tumors (**Table 1A,B**). Correlations were also identified in no-Mets, All, and Visceral +Bone groups of luminal or TNBC patients (**Table 1A,B**). In addition ERRα expression was not associated with LM in two cohorts of BCa patients (16). Thus, this set of data from human sample analyses strongly suggests that, similarly to mice, the over-expression of *ERRα* in human BCa cells allows them to create an immune-efficient environment in the bone by increasing the production of chemokines capable of attracting activated T cells to the bone and decreasing the production of TGF-β essential for repressing the cytotoxic activity of T cells.

Discussion

Cancer cells adapt to the microenvironment, shaped by their own doing, which in turn influence their fate. This interplay is particularly important for cells forming metastases, which leave their primary microenvironment to settled in a new, second one. Here, we revealed that the level of

ERRα expression on BCa metastases promotes their ability to condition an efficient anti-tumor CD8^{+} T cell response selectively in the bone.

CD8^{+} T cells have been described as critical inhibitors of bone metastases. Indeed, in mice, the alteration of CD8^{+} T cell development after metastases implantation in the bone, or the deprivation of CD8^{+} T cells, were reported to increase tumor growth (5)(6). Osteoclasts have been depicted to secrete chemokines that can attract CD8^{+}T cells (33). However, the regulation of the BM burden by CD8^{+} T cells seems totally independent of the osteoclast activity (6). Our study reveals that the cancer cells *per se* can influence both the recruitment and the cytotoxic activity of the CD8^{+} T cells in the bone. Moreover, the ability of the BCa metastases to condition the immune response in the bone can be in part orchestrated by the levels of expression ERRα on the BCa and potentially to the sensitivity of metastases to the ERRα ligand(s). The selective effects of ERRα expression in BCa on the tumor burden of BM and anti-tumor response in the bone strongly suggest that unlike the lung, the bone could constitute a microenvironment with high levels of the ERRα ligand(s) that so far remain uncharacterized. Another alternative is that in the lung, but not the bone could be highly enriched in inhibitors of ERRα signaling or negative regulators of ERRα expression that remain to be identified. Thus, the ability of the metastases to induce or not a potent immune response maybe dictated by both the tumor *per se* and the microenvironment where it is anchored. In the case of BCa cells, we propose to place ERRα at the core of this interplay between metastases and their new microenvironment

In addition to increasing the recruitment of activated CD8^{+} T cells to the bone, the over-expression of ERRα on BCa cells also decreased their ability to produce high amounts of TGF-β3. Depletion experiments confirmed that CD8^{+} T cells are key anti tumor immune cells whose activation and recruitment are controlled by the levels of ERRα expression on BM. All forms of TGF-β have been reported as potent immune-regulators and share a common receptor (34). While TGF-β1 is predominant in the immune system, TGF-β3 is mainly produced by muscles, bones

but also by various cancer cells (35). The repression of TGF-β3 production in ERRα BCa cells, subsequently affects TGF-β signaling in CD8^{+} T cells present in the bone. TGF-β signaling represses the expression of numerous transcription factors associated with cytotoxicity, as well as T-Bet a key inducer of IFN-γ (36). Therefore, over-expressed ERRα BCa cells that settle in the bone are unable to sustain an immunosuppressive microenvironment based on high levels of TGF-β signaling in T cells and repression of cytotoxic program and IFN-γ production. Interestingly IFN-γ also contributes to the suppression of BM. Indeed, IFN-γ has been reported to reduce both RANKL expression and osteoclast formation, counterbalancing the aberrant bone resorption which facilitates tumor growth (37). Concomitantly, inhibition of bone resorption also leads to the decrease in TGF-β release from the bone matrix (4), thus potentially contributing to amplifying the activation of T cells including their production of IFN-γ.

It is likely that effector CD8^{+}T cells that reach the BM have previously been primed in the draining lymph nodes or by the spleen-presenting antigens from the primary tumor and/or the metastases. As in the primary tumor, the activated CD8^{+}T cell population in contact with the BM is actually heterogeneous and composed of cells recently activated and activated memory cells. Interestingly, in both mice and humans, the fraction of CD8^{+}T cells that expresses CCR6 and CCR4 has been depicted to rapidly mount an efficient response, corresponding to activated /memory T cells (28). Once implanted in the bone, we found that the BCa over-expressing ERRα have unique ability to sustain high expression of CCL17 and CCL20 and low expression of TGF-β3, thus attracting the activated/memory CD8^{+}T cells whose their anti-tumor cytotoxic function is magnified by the lack of repression by TGF-β signaling.

In conclusion, this study assigns an unsuspected role for ERRα expression in BCa on the bone immune system that conditions the BM growth outcome, providing the mechanistic basis for understanding how ERRα expression in BCa can impact the bone microenvironment and reduce BM growth. ERRα seems to appear at the core of this interplay between BCa metastases and their

new environment, integrating signals from the microenvironment to develop an efficient anti-tumor response. Therefore, we propose to consider ERRα expression on BCa, as a biomarker predictive of BM response to immunotherapies and /or as a good prognosis marker in BM progression once established, opening the path towards to the clinical use of ERRα agonist to relieve patients with ERRα positive BM after primary tumor resection.

References

1.   Kan C, Vargas G, Pape F, Clézardin P. Cancer Cell Colonisation in the Bone Microenvironment. Int J Mol Sci. 2016 Oct 4;

2.   Croucher P, McDonald M, Martin T. Bone metastasis: the importance of the neighbourhood. Nat Rev Cancer. 2016 May 25;373–86.

3.   Handforth C, D'Oronzo S, Coleman R, Brown J. Cancer Treatment and Bone Health. Calcif Tissue Int. 2018 Feb;251–64.

4.   Esposito M, Guise TA, Kang Y. The Biology of Bone Metastasis. Cold Spring Harb Perspect Med. 2018 Jun 1;

5.   Bidwell B, Slaney C, Withana N, Forster S, Cao Y, Loi S, et al. Silencing of Irf7 pathways in breast cancer cells promotes bone metastasis through immune escape. Nat Med. 2012;1224–31.

6.   Zhang K, Kim S, Cremasco V, Hirbe A, Collins L, Piwnica-Worms D, et al. CD8+ T cells regulate bone tumor burden independent of osteoclast resorption. Cancer Res. 2011 Jul 15;4799–808.

7.   Mori G, D'Amelio P, Faccio R, Brunetti G. Bone-immune cell crosstalk: bone diseases. J Immunol Res. 2015;

8.   Pacifici R, Weitzmann M. Immunobiology and bone. In: Primer on the metabolic bone diseases and disorders of mineral metabolism. ninth. 2019. p. 992–1003.

9.   Ariazi EA, Clark GM, Mertz JE. Estrogen-related receptor alpha and estrogen-related receptor gamma associate with unfavorable and favorable biomarkers, respectively, in human breast cancer. Cancer Res. 2002 Nov 15;62(22):6510–8.

10.   Deblois G GV. Oestrogen-related receptors in breast cancer: control of cellular metabolism and beyond. Nat Rev Cancer. 2013;13(1):27–36.

11.   Audet-Walsh E, Giguére V. The multiple universes of estrogen-related receptor α and γ in metabolic control and related diseases. Acta Pharmacol Sin. 2015 Jan;36(1):51–61.

12.   Patch RJ, Searle LL, Kim AJ, De D, Zhu X, Askari HB, et al. Identification of diaryl ther-based ligands for estrogen-related receptor alpha as potential antidiabetic agents. Journal of medicinal chemistry. 2011 Feb 10;54(3):788–808.

13.   Willy PJ, Murray IR, Qian J, Busch BB, Stevens WC Jr, Martin R, et al. Regulation of PPARgamma coactivator 1alpha (PGC-1alpha) signaling by an estrogen-related receptor alpha (ERRalpha) ligand. Proc Natl Acad Sci U S A. 2004 Jun 15;101(24):8912–7.

14.   Tam I, Giguère G. There and back again: The journey of the estrogen-related receptors in the cancer realm. J Steroid Biochem Mol Biol. 2016 Mar;13–9.

15.   Dwyer MA, Joseph JD, Wade HE, Eaton ML, Kunder RS, Kazmin D, et al. WNT11 expression is induced by estrogen-related receptor alpha and beta-catenin and acts in an autocrine manner to increase cancer cell migration. Cancer Res. 2010 Nov 15;70(22):9298–308.

16.   Vargas G, Bouchet M, Bouazza L, Reboul P, Boyault C, Gervais M, et al. ERRα promotes breast cancer cell dissemination to bone by increasing RANK expression in primary breast tumors. Oncogene. 2019 Feb;950–64.

17.   Peyruchaud O, Winding B, Pecheur I, Serre CM, Delmas P, Clezardin P. Early detection of bone metastases in a murine model using fluorescent human breast cancer cells: application to the use of the bisphosphonate zoledronic acid in the treatment of osteolytic lesions. Journal of bone and mineral research : the official journal of the American Society for Bone and Mineral Research. 2001 Nov;16(11):2027–34.

18.   Fradet A, Sorel H, Bouazza L, Goehrig D, Depalle B, Bellahcene A, et al. Dual function of ERRalpha in breast cancer and bone metastasis formation: implication of

VEGF and osteoprotegerin. Cancer research. 2011 Sep 1;71(17):5728–38.

19. Patch R, Searle L, Kim A, De D, Zhu X, Askari H, et al. Identification of diaryl ether-based ligands for estrogen-related receptor alpha as potential antidiabetic agents. J Med Chem. 2011 Feb 10;788–808.

20. Bos P, Zhang X, Nadal C, Shu W, Gomis R, Nguyen D, et al. Genes that mediate breast cancer metastasis to the brain. Nature. 2009 Jun 18;1005–9.

21. Wang Y, Klijn J, Zhang Y, Sieuwerts A, Look M, Yang F, et al. Gene-expression profiles to predict distant metastasis of lymph-node-negative primary breast cancer. Lancet. 2005 Feb 19;671–9.

22. Minn A, Gupta G, Siegel P, Bos P, Shu W, Giri D, et al. Genes that mediate breast cancer metastasis to lung. Nature. 2005 Jul 28;518–24.

23. Pillich R, Chen J, Rynkov V, Pratt W, Pratt D. NDEx: A Community Resource for Sharing and Publishing of Biological Networks.

24. Pratt D, Chen J, Pillich R, Rynkov V, Gary A, Demchak B, et al. NDEx 2.0: A Clearinghouse for Research on Cancer Pathways. Cancer Res. 2017 Nov 1;:58-61.

25. Yevshin I, Sharipov L, Valeev T, Kel A, Kolpakov F. GTRD: a database of transcription factor binding sites identified by ChIP-seq experiments. Nucleic Acids Res. 2017;D61–7.

26. Deblois G, Smith H, Tam I, Gravel S, Caron M, Savage P, et al. ERRα mediates metabolic adaptations driving lapatinib resistance in breast cancer. 2016 Jul 12;12156.

27. Eskiocak B, Ali A, White. The Estrogen-Related Receptor α Inverse Agonist XCT 790 Is a Nanomolar Mitochondrial Uncoupler. Biochemistry. 2014 Jul 29;4839–46.

28. Ferguson A, Engelhard V. CD8 T cells activated in distinct lymphoid organs differentially express adhesion proteins and coexpress multiple chemokine receptors. J Immunol. 2010 Apr 15;4079–86.

29. Stark C, Breitkreutz B, Reguly T, Boucher L, Breitkreutz A, Tyers M. BioGRID: a general repository for interaction datasets. Nucleic Acids Res. 2006;

30. He X, He X, Dave V, Zhang Y, Hua X, Nicolas E, et al. The zinc finger transcription factor Th-POK regulates CD4 versus CD8 T-cell lineage commitment. Nature. 2005 Feb 24;826–33.

31. Marie J, Liggitt D, Rudensky A. Cellular mechanisms of fatal early-onset autoimmunity in mice with the T cell-specific targeting of transforming growth factor-beta receptor. Immunity. 2006 Sep;441–54.

32. Derynck R, Zhang Y. Smad-dependent and Smad-independent pathways in TGF-beta family signalling. Nature. Oct 9;425(6958):577–84.

33. Kiesel J, Buchwald Z, Aurora R. Cross-presentation by osteoclasts induces FoxP3 in CD8+ T cells. J Immunol. 2009 May 1;5477–87.

34. Chen W, Ten Dijke P. Immunoregulation by members of the TGFβ superfamily. Chen W1, Ten Dijke P2. Nat Rev Immunol. 2016 Nov 25;723–40.

35. Letterio J, Roberts A. Regulation of immune responses by TGF-beta. Annu Rev Immunol. 1998;137–61.

36. Oh S, Mo L. TGF-β: guardian of T cell function. J Immunol. 2013 Oct 15;3973–9.

37. Nagy E, Lei Y, Martínez-Martínez E, Body S, Schlotter F, Creager M, et al. Interferon-γ Released by Activated CD8+ T Lymphocytes Impairs the Calcium Resorption Potential of Osteoclasts in Calcified Human Aortic Valves. Am J Pathol. 2017 Jun;1413–25.

A

Correlation with *ESRRA*	All (N = 248) Luminal		No Mets (N = 121)		Visceral + Bone (N = 53)		Bone Only (N = 74)	
	R	P-value	R	P-value	R	P-value	R	P-value
CCL17	**0.4933**	< 0.0001	**0.2725**	0.0025	**0.4918**	0.0002	**0.5547**	< 0.0001
CCL20	**0.3145**	< 0.0001	**0.2209**	0.0149	0.2136	0.1246	**0.3058**	0.0081
TGFβ3	-0.449	0.0001	-0.215	0.0176	-0.448	0.0007	-0.428	0.0001

B

Correlation with *ESRRA*	All (N = 110) Triple negative		No Mets (N = 50)		Visceral + Bone (N = 53)		Bone Only (N = 16)	
	R	P-value	R	P-value	R	P-value	R	P-value
CCL17	**0.313**	0.0009	0.096	0.5038	0.254	0.0663	**0.648**	0.0067
CCL20	**0.272**	0.0040	0.190	0.1855	**0.332**	0.0153	**0.604**	0.0132
TGFβ3	-0.465	0.0001	-0.327	0.0201	-0.438	0.0010	-0.705	0.0022

Table.1

Table and Figure legends

Fig. 1: Inhibition of BM development by ERRα overexpression in BCa.

(A-N), 4T1-CT, 4T1-ERRα or 4T1-CT(af2) and 4T1-ERRαAF2 cells were inoculated into BALB/c mice. 13-15 days post-inoculation, osteolytic lesions were analyzed. **(A)** Representative radiography. The osteolytic regions are delimitated by dash lines. **(B)** Graphs illustrate the mean size (mm^2) ± SEM of osteolytic lesions (n=10 mice per group, Mann-Whitney, osteolysis: $P < 0.0001$: 4T1-ERRα *versus* CT). **(C, D)** Three-dimensional microCT reconstruction representation of tibiae in sagittal sections (C) and cross sections (D) following the cutting of the bone along the plane illustrated by the dashed lines in C. **(E)** Graphs illustrate the mean of the % of Bone Volume/Tissues Volume ± SEM (n=10, Mann-Whitney, BV/TV: $P < 0.0001$ for 4T1-ERRα *versus* CT). **(F)** Histological images of bone sections after Goldner's Trichrome staining. Tumors are delimitated by dash lines and * indicate the bone marrow. **(G)** Graphs illustrate the mean of % of Tumor Burden /Soft Tissues Volume ± SEM (n=10, Mann-Whitney, TB/STV: $P < 0.0001$ for 4T1-ERRα *versus* CT). **(H-N)** Respective representation and quantification of clones expressing a dominant-negative form (4T1-ERRαAF2) with their controls clones (4T1-CTaf2): osteolytic lesions (n=9, Mann-Whitney, osteolysis: $P < 0.0006$: ERRαAF2 *versus* CT (af2)) (H, I), % of Bone Volume/Tissues Volume ± SEM (n=9, Mann-Whitney, BV/TV: $P < 0.0006$ for 4T1-ERRαAF2 *versus* CT(af2)) (J-L) and % of Tumor Burden /Soft Tissues Volume ± SEM (n=9, Mann-Whitney, TB/STV: $P < 0.0002$ for 4T1-ERRαAF2 *versus* CT(af2)) (M, N).

Fig. 2: Overexpression of ERRα in BCa cells has no impact on lung metastases development.
(A) Histological analysis assessment of lung of mice 15 days post-cell injection after H&E coloration. Metastasis are marked with * **(B)** Graph illustrate the numbers of LM counted on 3 representative sections at different levels of deepness (n=6). **(C-F)** Lungs from the same mice used to quantify BM (Fig.1) were crushed and cells released were cultured for 2 weeks. **(C and E)** are

representative pictures of LM colonies and **(D and F)** are graphs that illustrate the mean of number LM colonies formed for all mice ± SEM (n=6, Mann-Whitney, TB/STV: *P*>0.05). **(G)** Graph illustrates the mean ERRα expression in LM cell colonies after 2 weeks of culture. Semi-quantitative PCR was performed in triplicate on n=3 animals (unpaired t-test: *P* < 0.0001) and normalized against the ribosomal protein gene *L32* (mean ±SEM).

Fig. 3: Overexpression of ERRα in BCa cells promotes CD8$^+$ T cytotoxic function.

Cells suspensions were prepared from metastatic legs (bone) (A, C, D-F) or lungs (B, C) of mice (n=4) inoculated with 4T1-CT or 4T1-ERRα cells. **(A-B)** Flow cytometry contour plots of CD45$^+$ hematopoietic cells, illustrating the proportion of T cells (CD3$^+$), B cells (CD19$^+$) and CD4/CD8 T cells and graphs representing the percentage of cells in the bone (A) (mean ±SD, n = 4, student t-test ** *P* < 0.001, *** *P* < 0.0001) and in the lungs (B). **(C)** Flow cytometry contour plots illustrating the production of FasL, LAMP-1, Granzyme A and B and IFNγ in CD8$^+$ T cells. **(D)** Graphs demonstrate the percentage of cells and **(E)** their absolute numbers. **(F, G)** Fluorescent micrographs of sections of 4T1-CT or 4T1-ERRα-expressing bone after *TUNEL* assay and enlarged views of dashed rectangles. Apoptotic cells are shown in red and the cell nucleus in blue after DAPI staining. (G, H) Scale bar=50μm, T: tumor, GP: growth plate with apoptotic hypertrophic chondrocytes indicated by white arrows.

Fig. 4: CD8$^+$ T cell depletion restore 4T1-ERRα BM progression.

4T1-ERRα cells injected mice were treated with anti-CD8 antibodies every two day once osteolytic lesions occur *ie* at day 10 based on radiograhy **(A)** Flow cytometry analysis confirming the CD8$^+$ T cell-depletion in the bones. **(B)** Radiography, illustrating representative osteolytic lesions 18 days post- 4T1-ERRα cells inoculation. The osteolytic regions are delimitated by dash lines. **(C)** Three-dimensional microCT reconstruction representation of tibiae in sagittal sections

(**C**) and cross sections (**D**) following the cutting of the bone along the plane illustrated by the dashed lines in C. (**E**) Graphs illustrate the mean of the % of Bone Volume/Tissues Volume ± SEM (Mann-Whitney, BV/TV: P =0.0037).

Fig. 5: Ccl17 and Ccl20 up-regulation by ERRα in BCa cells.

(**A**) Heat map representative of cytokine, chemokine and growth factor mRNA expression in 4T1-ERRα and 4T1-CT cells, normalized against *Ppia*, *Actb* and *Rplp0* expression. (**B-D**) Graph illustrates the relative gene expression after RT-PCR performed on triplicate samples and normalized against the ribosomal protein gene *L32* (mean ± SEM). (**B**) 4T1-ERRα, 4T1-CT or 4T1-ERRαAF2, 4T1-CT(af2) cells were analyzed (n=2, ANOVA: $P < 0.0001$ for *Ccl17* and *Ccl20*, unpaired t-test P=0.0007 (*Ccl17*), $P = 0.0005$ (*Ccl20*) (4T1-ERRα) and $P = 0.0004$ *(Ccl20)* 4T1-ERRαAF2 *versus* 4T1-CT). (**C-D**) 4T1-ERRα and 4T1-ERRαAF2 cells were cultured for 24 hours with the inverse-agonist C29 (5 μM) (unpaired t-test, $P = 0.0005$ and $P = 0.0034$ for *Ccl17* and *Ccl20*, respectively). (**E**) Tumor cell colonies obtained after crushing bones extracted from mice (n = 3) bearing either 4T1-ERRα or 4T1-CT lesions and cultured during 4 weeks were analyzed (unpaired t-test $P = 0.0059$ (*Ccl17*), $P < 0.0001$ (*Ccl20*) and $P < 0.0001$ (*ERRα*)). (**F**) Immunostaining for Ccl17 and Ccl20 on bone section colonized by either 4T1-ERRα or 4T1-CT cells. Bar = 200 μm, T: tumor, GP: growth plate. (**G**) Representative flow cytometry contour plot illustrating the expression of CCR4 and CCR6 on CD8^{+} T cells from bones colonized with either 4T1-ERRα or 4T1-CT cells. All *in vitro* and *ex vivo* analyses were repeated at least twice. Data are plotted as mean ± SEM.

Fig. 6: Over-expression of ERRα in BCa inhibits *Tgf-β3* expression and affects TGF-β signaling in CD8^{+}T cells. (A) Overlay of the Minimal Network (containing 101 proteins) with extracted information from the Gene-Ontology-consortium of proteins involved in the immune

system process, as well as to create "Minimal Network specific to immune response to tumor" (containing 52 proteins). **(B, C)** Potential new regulators of ESRRA, including VCAM1, MACF1, HUR and TGF-β3, were identified through systematic shortest path definition of crosstalks. **(D-E)** Graphs illustrating the relative gene expression after RT-PCR performed on triplicate samples and normalized against the ribosomal protein gene *L32* (mean ± SEM). **(D)** 4T1-ERRα, 4T1-ERRαAF2, 4T1-CT and 4T1-CT(af2) cells were analyzed (ANOVA: *P* < 0.0001 and unpaired t-test *P* < 0.0001 4T1-ERRα *versus* 4T1-CT, *P* = 0.0009 for 4T1-ERRαAF2 *versus* 4T1-CT(af2)). **(E)** Tumor cell colonies obtained after crushing bones extracted from mice (n = 3) bearing either 4T1-ERRα or 4T1-CT lesions and cultured during 4 weeks were analyzed (unpaired t-test *P* = 0.0056). **(F)** Immunostaining for *Tgf-β3* on bone section colonized by either 4T1-ERRα, 4T1-CT cells or 4T1-CT(af2) and 4T1-ERRαAF2 cells. Bar = 200 μm, T: tumor, GP: growth plate. **(G)** 4T1-ERRα cells were cultured for 24 hours with the inverse-agonist XCT-790 (1 μM) (unpaired t-test, *P* = 0.0007). Data are plotted as mean ± SEM. **(H)** RT PCR performed on mRNA of MCF7 and B02 clones. Mean of three different cultures for each MCF7 clones are shown for *TGF-β3* (unpaired t-test *P* = 0.0218 MCF7-ERRα *versus* MCF7-CT; B02 clones*: ANOVA: *P* = 0.0027, unpaired t-test *P* = 0.007: B02-ERRα v*ersus* B02-CT). **(I)** Representative flow cytometry histogram plot illustrating the phosphorylation of SMAD2/3 in CD8^{+} T cells from bones colonized with either 4T1-ERRα cells or 4T1-CT. The percentage of positive cells is illustrated. These *ex vivo* data are representative of 2 experiments with 3-4 mice per group. All *in vitro* analyses were repeated at least twice.

Table 1: Correlation in clinics in BCa patients. (A, B) Meta-analysis of public datasets (GSE12276-GSE2034-GSE2603) (n=248) revealed a positive correlation between the expression of *ESRRA* and *CCL17* and *CCL20* and a negative correlation with *TGF-β3* expression levels in luminal **(A)** and triple-negative **(B)** breast tumors. Correlation scores were

calculated using the Pearson correlation coefficient. P-values less than 0.05 were considered statistically significant.

Abbreviations used in this paper: ANOVA: analysis of variance; BM: Bone Metastases; B BV/TV: Bone Volume/Tissues Volume; CCL17-CCL20: Chemokine (C-C motif) ligand 17, 20; CCR4 and CCR6: C-C chemokine receptor type 4 and 6; ERR: estrogen receptor-related receptor; LAMP-1: Lysosome-associated membrane glycoprotein-1; LM: Lung Metastases; OCs: osteoclasts; RANKL: receptor activator of nuclear factor kB ligand; RT: reverse transcription; PCR: polymerase chain reaction; PMN-MDSC: Poly-MorphoNuclear Myeloid Derived Suppressor cells; TNBC: Triple-negative breast cancer; TGF-β: Transforming Growth Factor Beta; TB/STV: Burden /Soft Tissues Volume.
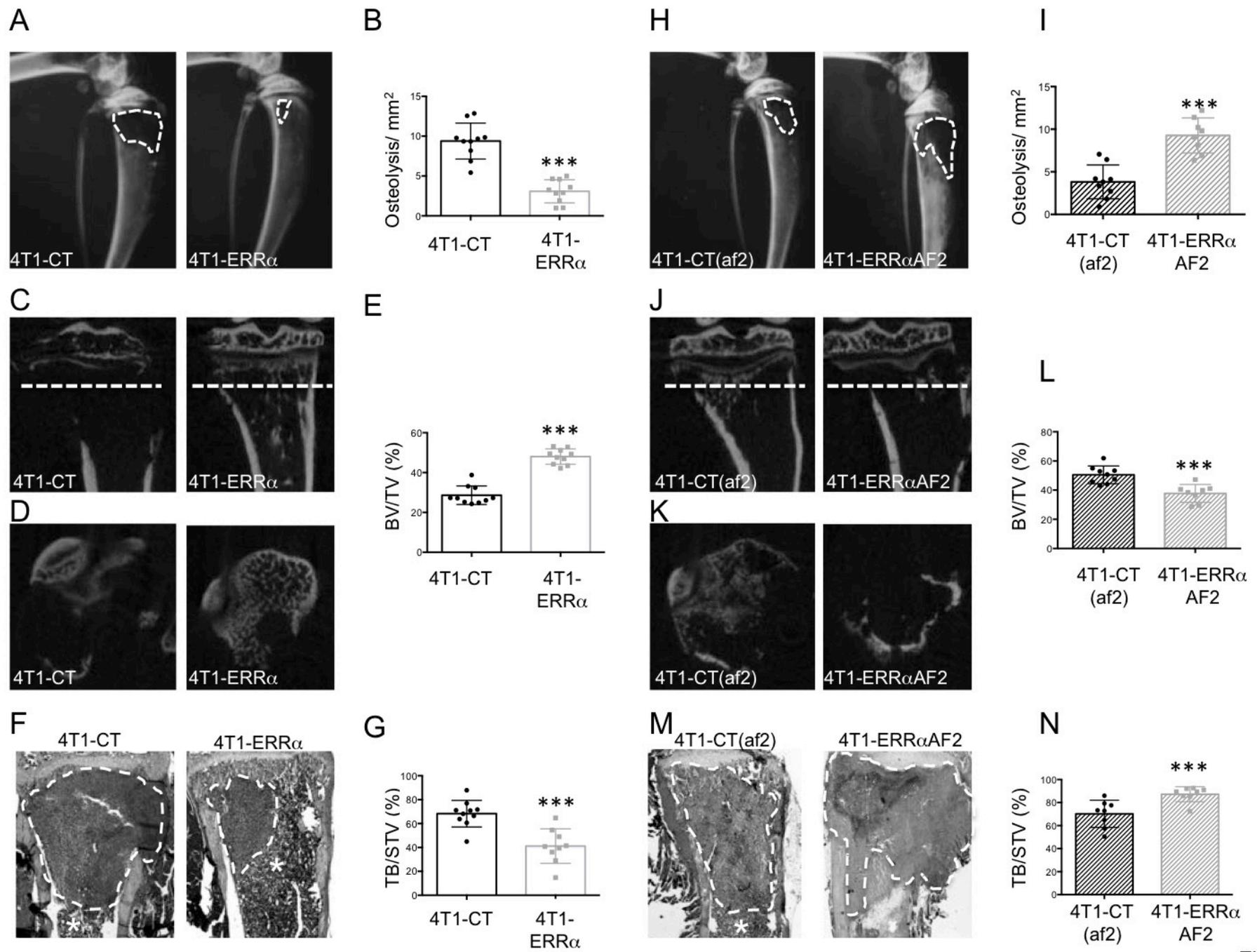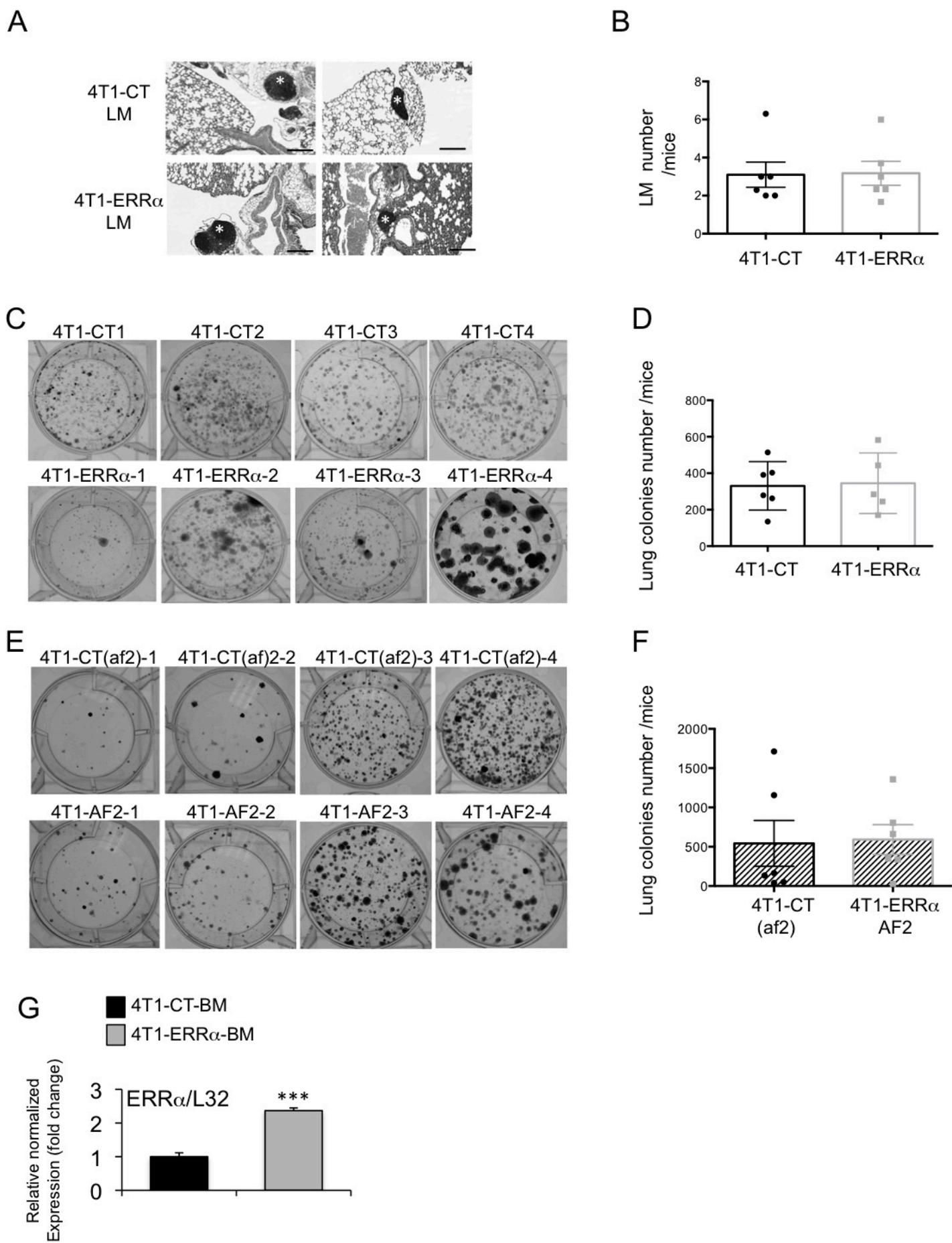
Figure.1

A

4T1-CT
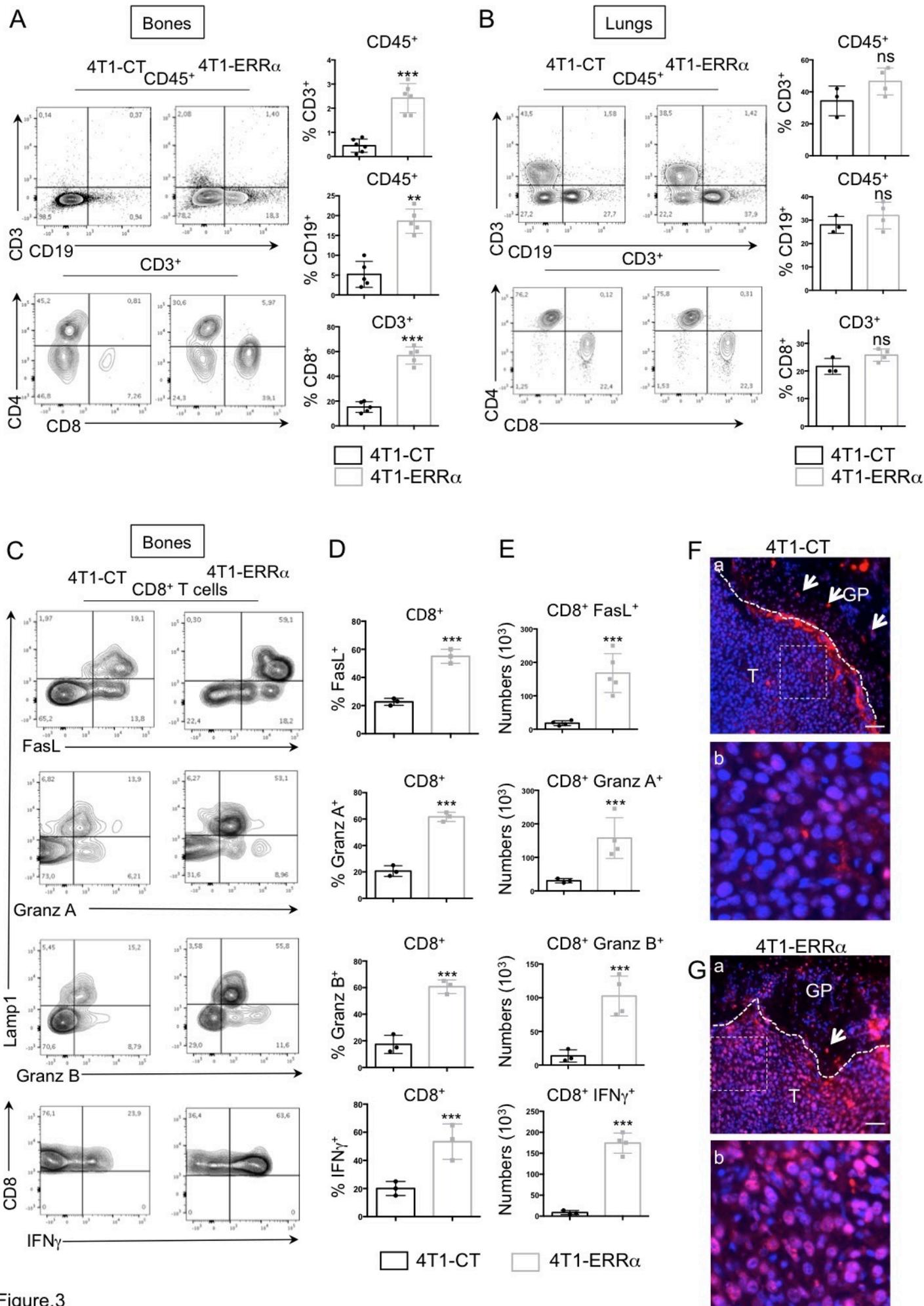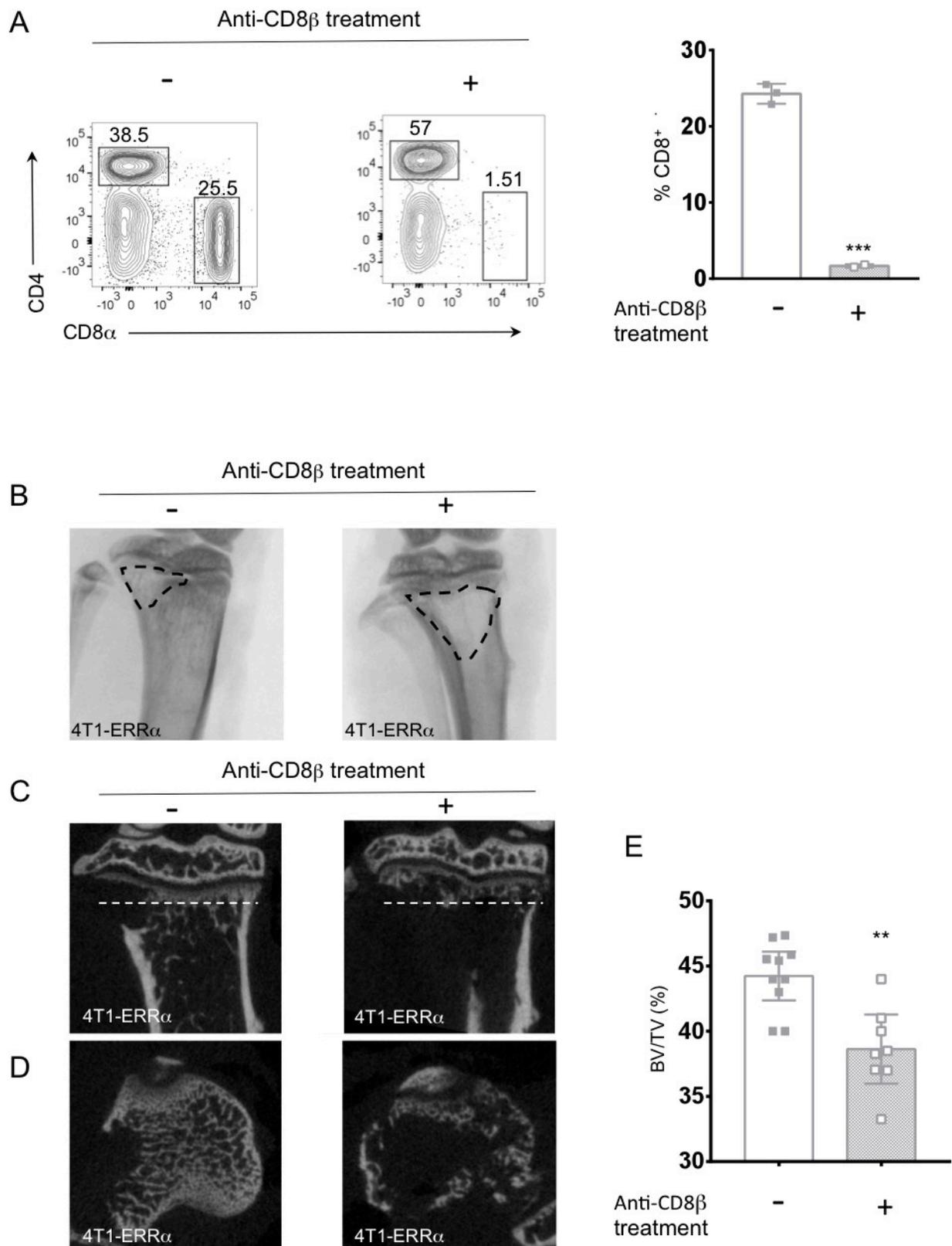LM

4T1-ERRα
LM

B

LM number /mice

4T1-CT   4T1-ERRα

C

4T1-CT1   4T1-CT2   4T1-CT3   4T1-CT4

4T1-ERRα-1   4T1-ERRα-2   4T1-ERRα-3   4T1-ERRα-4

D

Lung colonies number /mice

4T1-CT   4T1-ERRα

E

4T1-CT(af2)-1   4T1-CT(af)2-2   4T1-CT(af2)-3   4T1-CT(af2)-4

4T1-AF2-1   4T1-AF2-2   4T1-AF2-3   4T1-AF2-4

F

Lung colonies number /mice

4T1-CT
(af2)

4T1-ERRα
AF2

G

■ 4T1-CT-BM
■ 4T1-ERRα-BM

Relative normalized Expression (fold change)

ERRα/L32

***

Figure.2

Figure.3

Figure.4

Figure.5

Figure.6